



# A smart microfluidic-based fish farm for zebrafish screening

Karthick Mani<sup>1</sup> · Chia-Yuan Chen<sup>1</sup>

Received: 12 August 2020 / Accepted: 16 January 2021 / Published online: 12 February 2021  
© The Author(s), under exclusive licence to Springer-Verlag GmbH, DE part of Springer Nature 2021

## Abstract

Advances in microfluidics for zebrafish processing are critical to facilitate the bioassay in new drug development. Still, a manipulation platform for zebrafish relies mainly on the “static” agarose material and is coupled with the conventional fish facility to ensure the time-history investigation with the homogenous zebrafish population for drug screening. A fully automated IoT (Internet of Things) microfluidics system is necessary to be developed to enable smart and high-speed zebrafish testing without the need for fish facility support. In this work, a smart microfluidic device was presented to enable (i) highly efficient temperature control with the precision of  $\pm 0.1$  °C, (ii) remote zebrafish transport through light patterning, and (iii) perfusion and dynamic culturing of zebrafish all together assembled for on-chip high-quality imaging. A new microscale manipulation is envisaged to initiate a new chapter of running bioassays.

**Keywords** Microfluidics · Internet of things · Fish on a chip · Zebrafish · Automated drug screening

## 1 Introduction

Zebrafish as an animal model has been extensively employed for the study of vertebrate biomechanics, developmental biology, pharmacology, toxicology, genetic study, and cardiovascular development due to its experimental-friendly characteristics (Asnani and Peterson 2014; Dooley and Zon 2000). To access the important internal organs of this animal model, high-resolution imaging is required in which the zebrafish larvae are anesthetized and transported onto the imaging platform (Mani et al. 2016). Conventionally, zebrafish larvae are transported from the breeding environment to the imaging platform employing the mechanical pumping within the narrow capillary tubes or microchannels (Chang et al. 2012; Lin et al. 2015; Mani et al. 2016). Such a process may introduce serious damages to their fragile bodies. Although the research on the zebrafish-based organism model has achieved a remarkable progress, the manipulation platforms tailored for these zebrafish are still insufficient. As a result, a non-invasive method for larvae transportation is in high demand for medium-throughput particularly necessary to accelerate the embryo handling/manipulation and

the zebrafish-based drug development process (Wielhouwer et al. 2011). To meet these requirements, several special microfluidic platforms toward manipulation of zebrafish were developed such as a two-plate droplet-based “digital” microfluidic technology for on-chip transporting of zebrafish embryos (Son and Garrell 2009; Yang et al. 2016) and the shape memory-based Fish-Trap microchannel for real-time 3D mapping (Mani et al. 2016) together with artificial cilia-based micromanipulation platform (Chen et al. 2013) for zebrafish imaging with less detrimental effects on the larval growth (Chen et al. 2016). Still, the aforementioned microfluidic approaches can be further improved to effectively and anesthetic-freely transport zebrafish embryos (Mani et al. 2016; Zheng et al. 2014) to the desired positions accurately. Additionally, position-controlling the targeted zebrafish larvae with high precision is essential for high-resolution imaging. However, the rapid growth rate of zebrafish larvae poses a great challenge to assess during time-lapse imaging (Yang et al. 2016). For example, a drug screening procedure requires a high-accuracy imaging of larvae in time-history developing stages and dynamic culturing microenvironment is necessary to ensure an excretion-free physiological growing condition (Yang et al. 2016). An ingenious zebrafish transport system is, therefore, significantly needed to enable high-end applications.

Aside from it, studies have shown that for zebrafish to survive in a hostile environment and to find favorable

✉ Chia-Yuan Chen  
chiayuac@mail.ncku.edu.tw

<sup>1</sup> Department of Mechanical Engineering, National Cheng Kung University, No. 1 University Road, Tainan 701, Taiwan

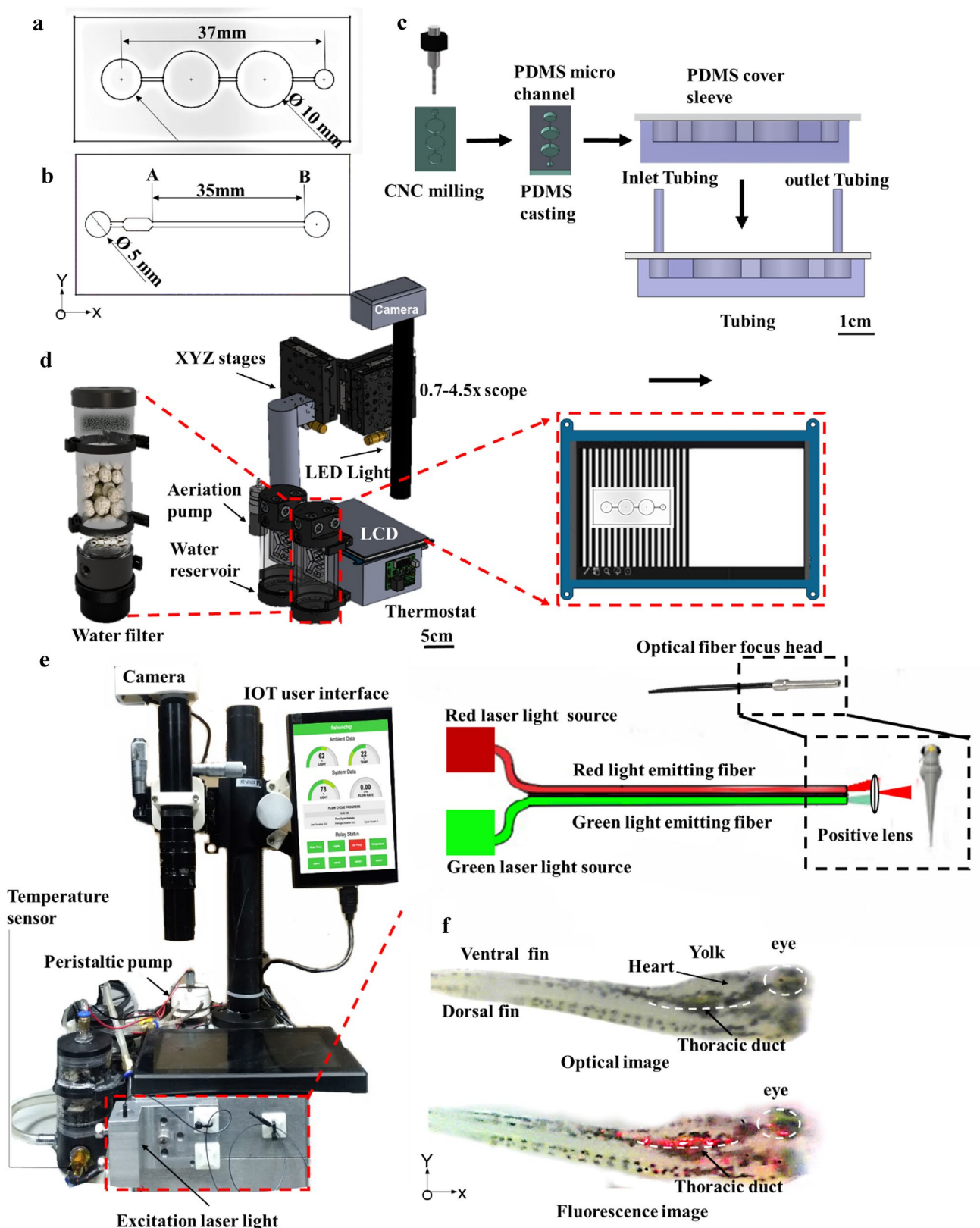


**Fig. 1** Schematic illustration of the experimental setup. **a** Dimensional details of the larvae culturing microchannel and **b** the microchannel to measure the transportation time required to move larvae from point A to B of larvae grown in the FF and PT groups. **c** The fabrication process of the microchannel. **d** The moving gratings were generated through the LED panel and the larvae were transported through the microfluidic network. The test zones for fish traveling time measurement through the stimuli from light patterns. **e** Image of the system equipped with sensors to provide a well-controlled environment for zebrafish and the laser excitation light source. **f** An fluorescence image of larvae with custom-developed fiber-optic laser excitation light

environments to collect their foods. One example is that the juvenile zebrafish larva can gather sensory and visual cues just 3 days post to their fertilization (days-post-fertilization, d.p.f.) (Neuhauss 2003; Schmitt and Dowling 1999; Wolf et al. 2017). The visuomotor behaviors in larval zebrafish can be broadly classified into two major categories such as optokinetic reflex (OKR) and optomotor response (OMR). OKR can be defined as a robust eye movement corresponding to a moving stimulus in the surrounding of zebrafish larva; whereas, OMR (Panigrahi and Chen 2019a) can be defined as the tendency of zebrafish larvae to follow the translational whole-field motion to stabilize their positions in the flow field. Although visuomotor behaviors of zebrafish larvae have been extensively studied and the considerable progress was made towards understanding the neural activity dynamics towards their innate responses, yet little attention has been devoted towards exploring its application side. As moving light grating can produce innate the optomotor behavioral response among juvenile zebrafish larvae and they can swim along the direction of perceived motion, a microfluidic device in conjunction with a light-driven technique was employed to transport zebrafish larvae within a microfluidic network to eliminate stresses related to manual handling (Mani et al. 2018) which provides a better alternative for zebrafish transportation within a microfluidic device.

To ensure the normal growth of zebrafish for the genetic screening with a homogeneous population, a well-controlled environment for zebrafish is necessary by filling the dynamic macroscopic water with oxygen, which is beneficial for timely dilution of excreta and replenishment of the culture media. In contrast, a traditional static platform like plastic multiwell plates or Petri dishes is incompatible with the requirements of dynamic culturing. In particular, the periodic aspiration and replacement of buffer are extremely invasive and can induce additional stress to the vulnerable embryos. Also, several other concerns regarding static exposure to zebrafish (eggs) need to be considered. One typical problem is the irreversibly gradual reduction of the exposed solution because of evaporation and nonselective adsorption, which leads to uncontrolled changes in concentration and the pH value of the original solution. One microfluidic flow-through system by providing non-invasive culture conditions

and accessibility to aid the normal dynamic growth of zebrafish embryos was developed which could yield a survival rate of 100% (Wielhouwer et al. 2011). This microdevice consists of two independent fluidic modes including an in-built micro-heating channel for circulating preheated water to ensure the desired temperature for embryo growth and a solution channel for continuous dynamic perfusion of on-chip embryos. The embryo-culturing chamber has a size (2.5 mm in diameter) much smaller than that of wells in conventional 96-well microliter plates (6 mm in diameter). Notably, the combination of biocompatible soft polymer material with a flexible channel-structure design endowed zebrafish an unstressed physiological growing environment. However, to develop a new generation of an “all-in-one” platform for on-chip larva trapping, culturing, exposing, analyzing, with fully automated control and monitoring functionalities is in urgent need.

On top of that, in terms of the microenvironment control system, a microfluidic chip should be designed in a way that includes the microfluidic network to grow embryos in the associated cultivation microchannel together with separately sorting and trapping sections to provide a comprehensive assessment of test zebrafishes with multi-functions. To further ensure the normal growth of the zebrafish within the microfluidic platform, key parameters of working fluid quality should be controlled specifically through the automatic system with high precision. These parameters are temperature, pH, salinity, alkalinity, hardness, dissolved oxygen, and nitrogenous wastes. The aforementioned parameters should have a preferred or optimum range of water quality parameters to ensure the normal development of zebrafish. The integration of the parameter control to a microfluidic network can provide a solid basis for precisely tuning the tailor-engineered micro-traps and a hydrodynamic (suction) “all-in-one” platform which is envisaged to enable the high-quality bio-test results for profound applications using zebrafish as an animal model.

## 2 Methods

### 2.1 Zebrafish transportation design

To evaluate the on-chip survival rate and development of the zebrafish larvae in the dynamic microenvironment supplied by the perfusion-style microfluidic dynamic culturing, two types of microfluidic devices were designed and employed for this fish farm. The design 1 microfluidic device was prepared for a microscale dynamic flow-through perfusion and culturing system (Fig. 1a), which consisted of incubation, observation, and culturing chambers. In design 2, (Fig. 1b) the microfluidic device consisted of a 35 -mm straight long channel with inlet opening for larvae loading.

The microchannel was first designed using a commercial software (Solid Works, Dassault Systèmes SolidWorks Corp., Waltham, MA, USA). Both designs 1 and 2 were fabricated by a series of micromachining and a mixture of PDMS and curing agent in a ratio of 10:1 were mixed uniformly, degassed in a vacuum chamber, and transferred into the acrylic mold. Successively, the whole assembly was placed on a hot plate at a temperature of 90 °C for a period of 10 h for the curing process. Afterward, the PDMS channel was separated from the mold, and an inlet and an outlet were punched. The microchannel was successively bonded with another PDMS layer through an oxygen plasma cleaning process. Polyethylene tubing (0.965-mm outside diameter (OD), 0.58-mm inside diameter (ID)) was employed to make the connection to the fish farm (Fig. 1c) components. Besides, approximately 90 eggs were collected in the morning and then divided into three groups with equal number of embryos. The temperatures of the three groups were set to ambient room temperature (P), 28.5 °C on temperature-controlled Petri dish (PT), and fish farm (FF), respectively (Fig. 3a). Embryos were selected at random, pipetted carefully into a respective dish and microfluidics. In the PT group, the water was partially replenished at every 48 h; while the larvae in the P group were not exposed to change in new media until 5 days. In the FF group, embryos were manually relocated into the incubation chambers and were exposed to slow-moving streams of the replenished water. All larvae used in experiments had not fed for at least 5 d.p.f. prior to experimentation to avoid bias in growth rate due uneven feeding between the larvae. Experiments were conducted at the same time each day (10 am) to prevent any diurnal effects. The survival rate was recorded by capturing the image using a camera positioned above the petri dish and microchannel. For growth measurement, a random selection of larvae ( $n=5$ ) from each group was carefully placed under the microscope for imaging at the same time each day (10 am). The selection of larvae with 3–5 d.p.f. was because at 3 d.p.f., all larvae in all three groups were hatched. Larvae were not handled manually by any means during the aforementioned test to unnecessary stress to the larvae (Fig. 3a). To invoke the OMR response of zebrafish larvae, the larvae were manually relocated into the incubation chambers by reversing the water flow, and inhouse developed animation pattern was played on the liquid crystal display (LCD) (Fig. 1d). The animation pattern was generated horizontally to the desired direction of transportation. Specifically, the microfluidic devices were aligned onto the generated light patterns as shown in (Fig. 1d). Note, the moving animation pattern on the bottom of the microfluidic device was tailored to fit specific microfluidic. The moving animation was played along the desired direction of zebrafish larvae transportation. The grating frequency and grating width ratio were set as 1.5 Hz and 1:1, respectively.

The movements of zebrafish larvae were recorded using a video camera mounted on a tripod holder. Recorded video files were replayed, and the larvae's activities were continuously tracked and recorded. The first experiment was intended to measure the time taken by larvae to swim from point A to B (35 mm) on design 2 (Fig. 1b). The response to visual stimuli was developed after 3 d.p.f. (Neuhauss 2003). As a result, a group of 5 d.p.f. zebrafish larvae was selected for the test in this study. To observe the responses of the zebrafish larvae to the artificial stimuli, a three-axis digital camera installed on the fish farm was used and the acquired videos were analyzed through an open-sourced tracker software (Schindelin et al. 2012). Embryos were not anesthetized to restrict their movement during imaging.

## 2.2 Fish farm

The automated fish farm system was individually controlled and optimized before final integration into the complete system, and an integrated three-axis microscope enabled the imaging of the assay. Although multiple imaging systems including confocal microscopy and 3D electron beam imaging have been successfully implemented for the microfluidic community, however, a low-cost alternative imaging system will become increasingly important for the whole-animal readout. The proposed system employed a relatively inexpensive LED with modified camera (C930e, Logitech, Switzerland) for imaging and the original optics on camera were replaced by Olympus C-Mount monocular video microscope tube 0.7–4.5X digital lens (Fig. 1d). An optical fiber (FU-10, Keyence International, Japan) with a 2-mm beam focusing was employed to avoid overexposing other larvae in the co-culture system. This arrangement can help reduce the induction of additional stress to larvae. In this setup, the laser was used as a light source with two different wavelength values, green (500–550 nm, H835151D/5D, Egismos laser diodes, Taiwan) and red lights (600–650 nm, H836351D/5D/10D, Egismos laser diodes, Taiwan) (Fig. 1e). The complete system was operated at 12 V, and the selected portable user-friendly microscope will allow for future on-site zebrafish monitoring. The sampled phenotype screening fluorescence images were taken as illustrated in (Fig. 1f). The life-support system consisted of several life-supporting devices (water purifier, temperature, and light management, liquid handling, automatic incubator, and the microscope) as illustrated in (Fig. 1d) which are critical to the growth dynamics of larvae and were individually controlled over the IoT (Internet of Things) server.

## 2.3 Drug preparation

Experiment was executed to showcase the drug testing capability of the fish farm system proposed in this study. This

experiment was designed to study the drug screening in real time, wherein the influences of a drug over the behaviors of the zebrafish larvae were measured in terms of the distance traveled by the larvae from point A to point B under an optical stimulus. It is well established that many drugs such as sedatives and anti-depressants that stimulate or suppress the central nervous systems (CNS) tamper with the motor activities of the larvae (Ruiz-Oliveira et al. 2019; Stewart et al. 2011; Vestergaard 2008). As a consequence, the behavioral responses of zebrafish larvae for moving graphics are affected considerably under the influence of CNS drug. Therefore, measuring the motor activity of the larvae will provide valuable insights into the effect of the drug on zebrafish behavior and motor responses, thus becoming an efficient tool for low-volume drug screening at an early stage.

The caffeine solution was prepared by mixing 94.6 mg of caffeine (Nasco, SA09406) with 200 ml of DI water which is the same dosage of caffeine presented in the average cup of coffee. This solution was further diluted into two different concentrations (1:10 and 1:20) using DI water before treatment. The treatment was then performed by exposing zebrafish larvae in a caffeine solution for 20 min through the infusion of caffeine in the upstream water flow, and the water returning from microchannel downstream was partially disconnected from the water filtration system before the experiment to avoid contamination of the fresh water by the drug in the fish farm system. A standard 168 mg/L tricaine buffer solution was prepared which was then diluted with DI water before the experiment. The tricaine buffer solution was infused in the same way as the caffeine in the caffeine experiment.

A liquid handling system featured independently filtering and replenishment components. For example, the filtration component was designed for providing continuously dynamic perfusion of on-chip embryos to facilitate real-time removal of the discharge waste from the larvae. In addition, a built-in closed-loop with 12-V and 40-W micro-heating systems were designed with a temperature sensor (TMP36, Analog Devices, USA) that can measure a wide range of temperature ( $-50$ – $125$  °C), with a precision (0.1 °C resolution) to ensure the desired water temperature for embryo growth. A micro-peristaltic pump with an integrated water flow sensor (SEN-HZ06S, Saier sensor Co., Ltd, China) was used which can be operated at a flow rate of 1 mL/s to produce positive pressure at the inlet of the microchannel. On top of it, a clogging sensor together with a one-way check valve was connected at the outlet of the pump to prevent the reverse flow. Finally, the oxygenated heated water flowed through the solenoid valve with sets of four micro-solenoid valves (SF-02, fspumps, China) connected to the IoT hardware to allow the end-users to connect up to four independent microchannels through the GUI. The light

exposure control system included two light sensors (GL55, Nanyang Senba Optical And Electronic Co., Ltd, China). The first sensor was placed on top of the fish farms microscope to acquire fish farm ambient light (Fig. 1d), and the second light sensor was positioned close to the microchannel which measured the light exposure of the larvae. The desired temperature/light/flowrate was specified as a reference value (Fig. 2b) to the PID control system. The water temperature inside the reserve tank was measured by a temperature sensor (TMP36, Analog Devices, USA) which was compared to the reference temperature for a stable PID control. The PID controller gave the PWM output to a MOSFET, and the desired optimal parameters of the PID controller were achieved by proper correction of proportional, integral, and derivative gain values ( $K_p$ ,  $K_i$ ,  $K_d$ ). The closed-loop PID control structure employed for the system is shown in (Fig. 2a). Also, if the ambient light was strong enough, the system light was then cut off. An aeration pump can be turned on or off by system settings, and the heater can be turned on if the temperature goes below the user-defined value (Fig. 2b). The circuit was completely isolated from the raspberry pi circuit using an eight-channel solid-state relay module with optocouplers. The aforementioned setting and controls are illustrated in Fig. 2a.

## 2.4 IoT system: monitoring and settings

A raspberry pi computer was set up to run the IoT server on a local area network. The webpage with graphical user interface (GUI) displayed the sensor data and also enabled end-users to change fish farm settings. The sensor data were updated at 10 Hz using WebSockets (Fig. 2b). The fish farm has sets of sensors for monitoring ambient, and the fish farm life-support system with real-time information was displayed on the GUI. The real-time flow rate of fluids through the system was displayed on the GUI as a flow gauge in liters per minutes. The system status such as water heater, water pump, aeration pump, and the light were indicated with color codes where the red color represented offline status; whereas, the green color represented the online status (Fig. 2b). All the processes were logged and displayed all the information of the system on GUI with system alerts. A flow cycle log can be readout for display information of the last cycle duration, the average cycle duration, and the total number of cycles during the operation. The flow log can be reset manually after each test. In terms of the system setting for the light control, the end-users can define wake/sleep cycles and minimum light (%) exposure. For the water pump, the end-users can set a value for liters per cycle and the number of pause beak in each cycle. The pulse break is beneficial as the flow can be temporarily paused during the imaging or drug infusion. For the temperate control, the end-users can define maximum temperature. In a case where

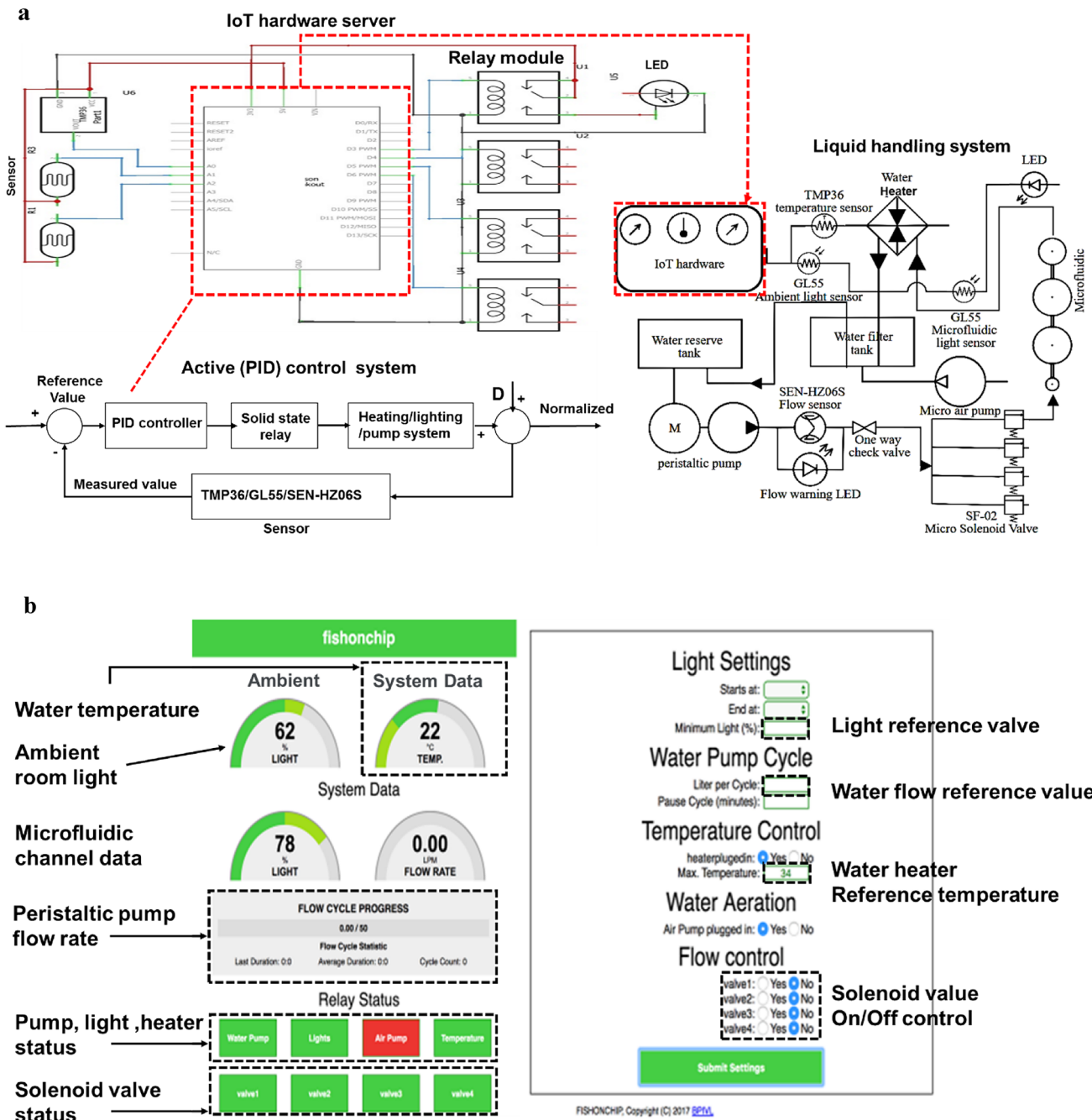


**Fig. 2** The IoT hardware and software system for the automated fish farm. **a** Schematics of the control flow chart and the fluid flow. **b** The schematic illustration of the graphical user interfaces for acquiring real-time sensor data

the ambient temperature goes below the reference value, the heater will be turned online. Finally, the air pump can run steadily which can be turned online or offline based on users' preference. In a special case when water is not flowing through the system due to water pump malfunction, an alert warning can be observed through LED lighting. Similarly, when system light fails and the system is not getting minimum set light, an alert LED will light up.

### 2.5 Statistics

The statistical significance of the groups in terms of zebrafish growth, survival rate, and manipulation was calculated based on the ANOVA test, Paired Student's *t* test, and Mann–Whitney test. The data normality was assessed by the Kolmogorov–Smirnov test.

**a**

Group		Petri dish (P)	Temperature controlled Petri dish (PT)	Fish farm (FF)
Sample size (N)		30	30	30
Environment control	Temperature	24-26°C	28.5°C	
	Perfusion	No		Dynamic perfusion
	Light	14 hours dark- 10 hours bright	12 hours dark- 12 hours bright	
Fish feeding		3-7 dpf		

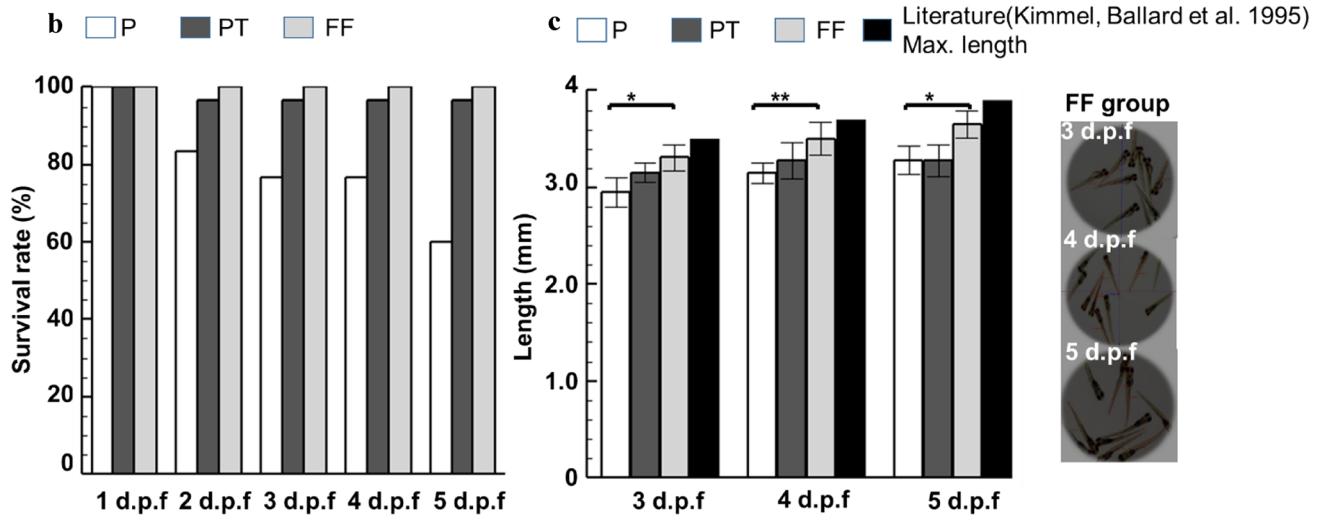


**Fig. 3** Zebrafish embryos obtained from spawning wild-type fish maintained at 28.5 °C were randomly assigned to three groups and incubated at room temperature petridish P (24–26 °C), temperature-controlled petridish PT (28.5 °C), and the fish farm FF (28.5 °C) (incubation temperature) throughout embryonic development. **a** The experimental matrix is shown for the test arrangement with represent-

ative culturing conditions. **b** The mortality rate of larvae during the growth 1–5 d.p.f.  $N=30$  fishes of three groups. **c** The average length of larvae of three groups compared with a maximum length of larvae report in the literature growth.  $N=5$  fishes \* $p$  value  $<0.01$  and \*\* $p$  value  $<0.05$  for the one-way ANOVA

### 3 Results and discussion

Initially, the proposed fish farm system was compared to conventional culturing methods to demonstrate its potentials for further drug screening. Specifically, in the FF group, zebrafish larvae were exposed to the constant dynamic perfusion through positive upstream medium generated by a peristaltic pump as opposed to those in the P and PT groups where the fluid was stationary. In addition, as known that larvae can display thermal plasticity during early embryonic development (Condon et al. 2010; Schaefer and Ryan 2006; Scott and Johnston 2012), and the performance of larvae at that particular temperature tends to improve compared to that of larvae exposed to other temperature conditions. The survival rate of larvae corresponding to the change in incubate temperature was verified. The data were then recorded by taking a time-lapse image every 24 h for 5 days, and the alive larvae were counted and documented. It indicates that the

lower temperature negatively affected the larvae during their embryonic development. In the early developmental stage, the survival rate of larvae originating from the incubation temperature range of 24–26 °C (P) was lower (60%,  $n=30$ ) after 5 days of fertilization (Fig. 3), and the temperature-controlled Petri dish group (PT) yielded 96.6% ( $n=30$ ) survival rate where the fish farm (FF) gave the 100% ( $n=30$ ) survival rate. In previous studies, they suggested that the inborn immune system was adversely affected by the low incubation temperature (Yang et al. 2016; Zhang et al. 2018), and the present system provided an ideal culture environment for zebrafish screening. Additionally, to identify the effect of the culturing temperature on the growth of zebrafish larvae in a quantitative manner, the length of the larvae was measured in all group during development stages. In the P group, the length was reported (Fig. 3) as  $2.95 \pm 0.17$  mm ( $n=5$ ) for 3 d.p.f. and it was  $3.28 \pm 0.16$  mm ( $n=5$ ) for 5 d.p.f. In the PT group it was  $3.28 \pm 0.18$  mm for 5 d.p.f. The best growth

rate was found in the FF group which are  $3.31 \pm 0.15$  mm and  $3.66 \pm 0.15$  mm for 3 d.p.f. and 5 d.p.f., respectively. These values also close to the maximum length of zebrafish grown in wild which are 3.5 and 3.9 mm (Kimmel et al. 1995), respectively. Furthermore, aforementioned results have statistically significant differences in the larvae growth rate between groups ( $*p$  value  $< 0.01$ ,  $**p$  value  $< 0.05$ ). Aside from the temperature control, the dynamic perfusion is also pivotal to the stage-specific larvae culturing system, which was evidenced by the larvae in the FF group expressing a slightly higher survival rate and growth compared to larvae raised in similar temperature of the PT group. Predominant factors such as temperature, light, and water quality can alter zebrafish physiological conditions especially in the early development stages which indicates a fact that there is a need to provide a comprehensive system to provide zebrafish-favorable conditions. In this sense, the microfluidic perfusion design is an ideal candidate providing non-intrusive culture conditions and convenience to aid the natural dynamic growth of zebrafish larvae during early embryonic development. In the present microfluidic device included in the fish farm, the culturing chamber has a size (10 mm in diameter) which is also sufficient for the well-hatched larvae to be transported automatically using the visual cue, and such a small culture volume can be beneficial for low-volume drug testing by saving valuable drug. Unfortunately, some time bubbles formed inside the microchannel which

reduced the efficiency of the dynamic flow-through system. To avoid the restrained bubbles, the channel outlets were slightly elevated than inlets to remove the air bubble through solution circulation.

To further verify the physiological performance of zebrafish larvae in FF and PT groups, the translational behaviors were depicted under the light stimulus. In the tests, the transporting time of zebrafish larvae was measured to represent the response of larvae's physiological behaviors, and is illustrated for two groups in Fig. 4a. Specifically, when the zebrafish larvae were introduced to the microchannel through the underlying moving black and white light patterning, larvae can move in the same direction as the moving patterning animation. This behavioral response of larvae to the external optical stimulus is known as the optomotor response (OMR) (Mani et al. 2018). The optimal behavioral responses of the larvae were measured when the animation has a spatial frequency of 1.5 Hz and the black/white animation has a width ratio of 1:1 which was reported in previous studies that also highlighted the incapability of larvae to follow the fast-moving visual stimuli due to the aliasing issues (Mani et al. 2018; Neuhauss 2003). With the optimal parameters, i.e., a spatial frequency of 1.5 Hz and the black and white animation width ratio of 1:1, the measurement was performed to document the required time frame for zebrafish larvae to move from point A to point B (35 mm). The traversing time of larvae was quantified by averaging the obtained period over total trials ( $n = 5$ ). To

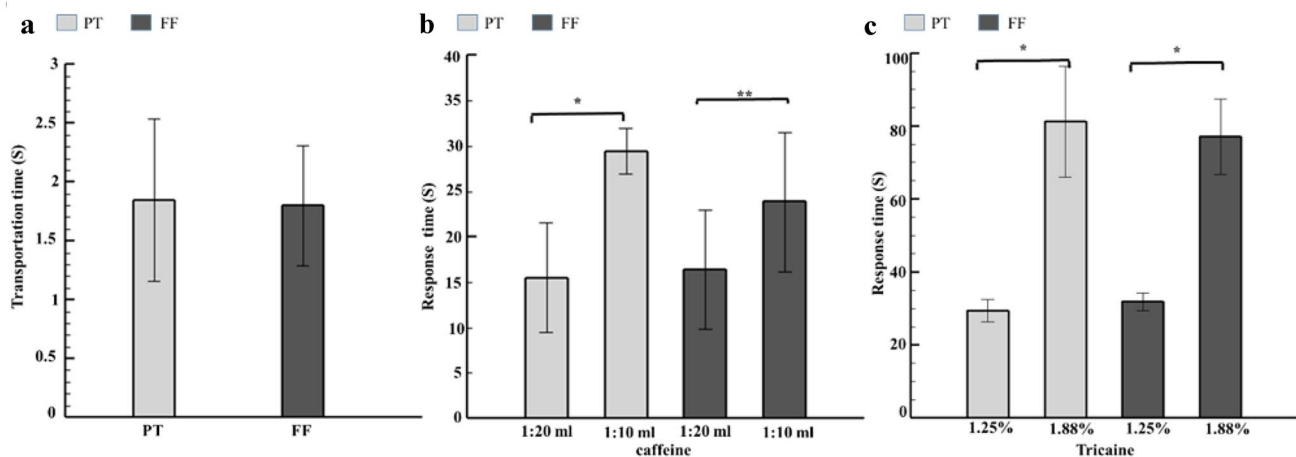


**Fig. 4** Drug testing capability of the proposed fish farm system. Fertilized zebrafish embryos were randomly assigned to two groups for incubation throughout embryonic development including the petri dish and the microchannel. Fishes were kept in Petri dishes (PT) at a density of 30 fish per dish and in the FF group, it was 10 fishes per microchannel. During the operation time, the circulating system that continuously filtered and aerated the system water to maintain the water quality required for a healthy aquatic environment. The circulating system also helped to filter fish excreta in the FF group,

while media was replaced once a day in the PT group. **a** The average traversing time required by the larvae to move from point A to B (35 mm) through the microchannel between the PT and FF groups,  $N = 5$  fishes. **b** The average traversing time required to move the larvae under the influence of the caffeine, and **c** the average traversing time required to move the larvae under the influence of a sedative tricaine,  $*P$  value  $< 0.01$  for the Mann–Whitney test,  $**p$  value  $< 0.05$  for the Wilcoxon Signed Ranks Test between PT and FF group,  $N = 5$  fishes



delineate the significance of the larvae responses throughout the tests, an unpaired sample Student's *t* test was performed. The maximum periods for 5 d.p.f. zebrafish larvae to swim 35 mm in the microchannel (design 2, Fig. 1b) were accounted as  $1.85 \pm 0.69$  s (mean  $\pm$  S.D.,  $n = 5$ ) and  $1.80 \pm 0.51$  s (mean  $\pm$  S.D.,  $n = 5$ ) for the PT and FF, respectively. The FF group was marginally higher than that of the PT group illustrated in (Fig. 4a). Results show that there was no significant difference in the optomotor swimming behavior of the larvae between both groups. The distance traveled by zebrafish larvae in terms of time for visual stimuli was highly depending on larvae's physical performance, and therefore the fish farm discussed in this study can serve as a better stage-specific system for the farming of zebrafish larvae. As noted in several of the previously published studies, zebrafish as a biomedical model is gaining enormous attention in toxicology (Harper and Lawrence 2010; Lawrence 2007; Panigrahi and Chen 2019b); however, it is also important to take into account that several factors such as temperature, light, water quality (acidity and alkalinity) (Blaser et al. 2010; Cortemeglia and Beiting 2005; Emran et al. 2008; Sawant 2011; Villamizar et al. 2014) tend to alter zebrafish behaviors. Populations exposed to different environmental conditions have been found to differ in the types of information they use to solve spatial tasks—fish from unstable river habitats rely less on visual cues than fish inhabiting visually stable habitats such as ponds (Agrawal 2001; Engeszer et al. 2007). Similarly, there are convincing findings about behavioral plasticity as an agent of micro- and macroevolutionary changes (Via and Lande 1985; Marks et al. 2005). It is believed that larvae under different conditions may respond differently to visual cues. Therefore, it is critical that the behavioral studies on lab-cultured zebrafish should be done in an environment which is fairly comparable to their natural environment. Still, it is unclear to what extent the above-mentioned factors affect the physiological/behavioral changes of the lab-cultured zebrafish fish larvae. To address these inadequacies, we proposed that the employment of the presented fish farm system which can precisely control the microenvironment within the fish farm thereby closely mimicking the natural environment, and as a result, significant biological effects on zebrafish behavioral endpoints can be avoided (the FF group).

In our study, the CNS drugs such as caffeine and tricaine were selected. Caffeine is a well-known CNS stimulant and is also widely used in foods, beverages, and medicines which are consumed by the people of all ages. However, at lower levels, caffeine can make people feel more alert and energetic, while a higher dose can cause a number of side effects including nervousness and difficulty in concentration. Also, it is well known that the effect of caffeine varies with body weight and the age of consumers. In the present study, the concentration of caffeine used for treating

the zebrafish was selected based on the average higher-level of caffeine consumed by human adults (Steele et al. 2018). The behavioral responses of larvae were then measured and documented as a function of the total time taken for the larvae to swim a fixed distance of 35 mm from the point of initiation of stimuli. The response time was quantified by averaging the acquired time over the total trials ( $n = 5$ ). It was found that the response time was minimum at a lower dosage of caffeine which demonstrated that the zebrafish locomotor response was very sensitive to caffeine. For example, at 1:20 dilution, the caffeine solution affected the startling behavior of larvae by decreasing the locomotor activity of the zebrafish larvae compared to the control group Fig. 4b ( $16.40 \pm 7.82$  s, mean  $\pm$  S.D.,  $n = 5$ ) and ( $15.51 \pm 5.89$  s mean  $\pm$  S.D.,  $n = 5$ ) for the FF and PT groups, respectively. At the dose of 1:10 dilution, the time taken for the locomotor activity was higher for the PT group ( $29.45 \pm 2.43$  s, mean  $\pm$  S.D.,  $n = 5$ ) in comparison with the FF group ( $23.83 \pm 9.23$  s, mean  $\pm$  S.D.,  $n = 5$ ) (Fig. 4b). Furthermore, the Mann–Whitney test (PT group,  $p$  value  $< 0.01$ ) and Wilcoxon Signed Ranks Test (FF group,  $p$  value  $< 0.05$ ) was performed based on the normality of the data, illustrated a statistically significant difference in the traversing time between the dosage of 1:10 and 1:20 under the optomotor stimuli. However, our findings in the present study suggested that, although exposure to caffeine significantly reduced the optomotor response of larvae to optical stimuli compared to untreated group, any dose higher than the 1:10 dosage showed no response to the stimuli.

Tricaine methanesulfonate, commonly called as Tricaine, is a well-known sedative which is widely used for the establishment of clinical level anesthesia for zebrafish (Mani et al. 2016). However, several publications have reported the side effects caused by tricaine including cardiac failure and death which depend on the dosage and exposure time (Li et al. 2014; Mani et al. 2016; Yang et al. 2016; Zheng et al. 2014). In addition, the negative side effects of Tricaine on behavior changes of zebrafish is not clear. In our system, we performed the behavior tests to determine whether or not tricaine affects the optomotor behavior of zebrafish larvae when treated with a lower dose. Similarly, the response time was also quantified by averaging the acquired time over the total trials ( $n = 5$ ). It is well established that while higher dosages of tricaine immobilize the larvae, the lower dosages do not eliminate the optomotor response of the larvae. For example, a dose of 1.25% of tricaine buffer in DI water showed a decrease in the activity under optomotor stimuli ( $31.87 \pm 2.49$  s, mean  $\pm$  S.D.,  $n = 5$ ) and ( $29.45 \pm 3.01$  s, mean  $\pm$  S.D.,  $n = 5$ ) for the FF and PT groups, respectively, whereas those treated with a slightly higher dose of 1.88% recorded higher time to the travel the same distance as that of 1.25% ( $77.03 \pm 10.36$  s, mean  $\pm$  S.D.,  $n = 5$ ) and ( $81.17 \pm 15.20$  s, mean  $\pm$  S.D.,  $n = 5$ ) for the FF and PT

groups, respectively (Fig. 4c (Neuhauss 2003)). Furthermore, the Mann–Whitney test further illustrated a statistically significant difference in the traversing time between the dosage of 1.25 and 1.88% under the optomotor stimuli (Mann–Whitney test,  $p$  value  $< 0.01$ ). In addition, the locomotor activity of the larvae treated with tricaine was sluggish as compared with the untreated larvae. Interestingly, while a low-dose tricaine decreases locomotor response, a high-dose tricaine tends to act as a CNS depressant which suppresses the response of zebrafish to the optomotor stimuli.

Zebrafish larvae can be traversed from one section to different sections of the microchannel with optical stimuli (Mani et al. 2018), however, the imaging platform has a fixed axis which made it difficult for imaging the free-swimming larvae. Therefore, a novel method was required for the orientation control of the larvae to the camera axis for automated or semi-automated imaging. Hence, fish experiments were conducted in the FF microfluidic test sections with two different sizes. The stereotyped eye movements of the larvae in response to the movements of any object in the field of vision is known as optokinetic (OKR) response. Interestingly, OKR helps zebrafish in its three-dimensional orientation, food hunting, and the escaping from predators. Zebrafish larvae develop an OKR response by 4 d.p.f. (Brockerhoff 2006), and this response can be precisely measured. Furthermore, this behavioral response is directly related to zebrafish brain development. In this test, 5 d.p.f. fishes were employed to avoid discrepancies related to zebrafish feeding since 5 d.p.f. larvae are not affected by feeding. To measure the zebrafish OKR, the microchannel was placed on top of LCD. The OKR response was then induced in zebrafish larvae with the help of an animation played on the LCD panel (Fig. 5a). The animation contained a 12-segment sunburst black and white graphics with a sequential frequency of 1.5 Hz, and it had a circular movement about the z-axis. After the animation started playing, the OKR response from the larvae was recorded at 30 fps. The recorded video was then imported into an open-source object tracking software TRACKER. Two points were selected and traced in the recorded video thorough the length of each larva, where one point was selected in between the zebrafish eyes which represented as a circle and the second point was 1.5 mm away from the first point on the dorsal fin which represented as a diamond (Fig. 5c). Results show that during the OKR response, the time taken by the larvae to traverse along the rotational direction of the stimulus generated was  $14.64 \pm 4.85$  s (mean  $\pm$  S.D.,  $n = 5$ ) for one complete axial rotation in a 10-mm microchannel. And the time taken for one complete axial rotation for a 5-mm channel was  $7.60 \pm 1.09$  s (mean  $\pm$  S.D.,  $n = 5$ ) (Fig. 5b). Furthermore, the paired student's  $t$  test illustrated a statistically

significant difference in the axial rotation time between the 5- and 10-mm microchannel test sections (paired sample  $t$  test,  $p$  value  $< 0.05$ ). Notably, as illustrated in the (Fig. 5c), the tracking results for the 5-mm microchannel showed that the diamond points were clustered in the center of the microchannel whereas the circle points were evenly distributed along the circumference wall of the microchannel. However, the tracking results for the 10-mm microchannel showed that both the circle and diamonds points were evenly distributed around the circumference of the microchannel wall (Fig. 5d). Notedly, when presented with a horizontal graphics motion, the larvae responded with a startling behavior. On the contrary, when presented with a rotational graphics motion, surprisingly, the larvae responded by traversing along the rotational axis, which was observed in all larvae in the sample group ( $n = 5$ ). In the 10-mm microchannel, the possible reason why the larvae tend to move closer to the walls of microchannel might be that they were traversing with an instinct which made them display a preference to stay close to the walls. Typical microscope systems used for the imaging of zebrafish larvae involved a labor-intensive manual procedure to orient the larvae to the desired orientation for organ-specific imaging (Yang et al. 2016). The proposed method in this study involved changing the size/dimension of the microchannel which resulted in the OKR response-mediated self-orientation of the larvae to the camera axis, thereby eliminating the need for labor-intensive human intervention. Still, a follow-up comprehensive study focusing on the geometry design of microchannel to the fish responses can provide a valuable tool for the automated imaging of the larvae. In addition, in terms of the orientation control during imaging, the presented experimental setup can also be utilized for the documentation of time-dependent responses observed in neurological studies.

## 4 Conclusion

This study demonstrated the importance of an autonomous microfluidic system that can accommodate the rapid growth rate of the zebrafish larvae, and also validated the fish growth parameters in the microfluidic channel platform through the precise control of temperature, light, and oxygenated water which can yield a better survival rate and a higher growth rate of  $3.7 \pm 0.15$  mm. at 5 d.p.f. This presented experimental setup and protocol can be further employed for drug screening; meanwhile, neurological behavioral screening as well as non-invasive automated transportation and orientation of larvae for imaging eliminated manual handling of test biosamples for more accurate measurements.

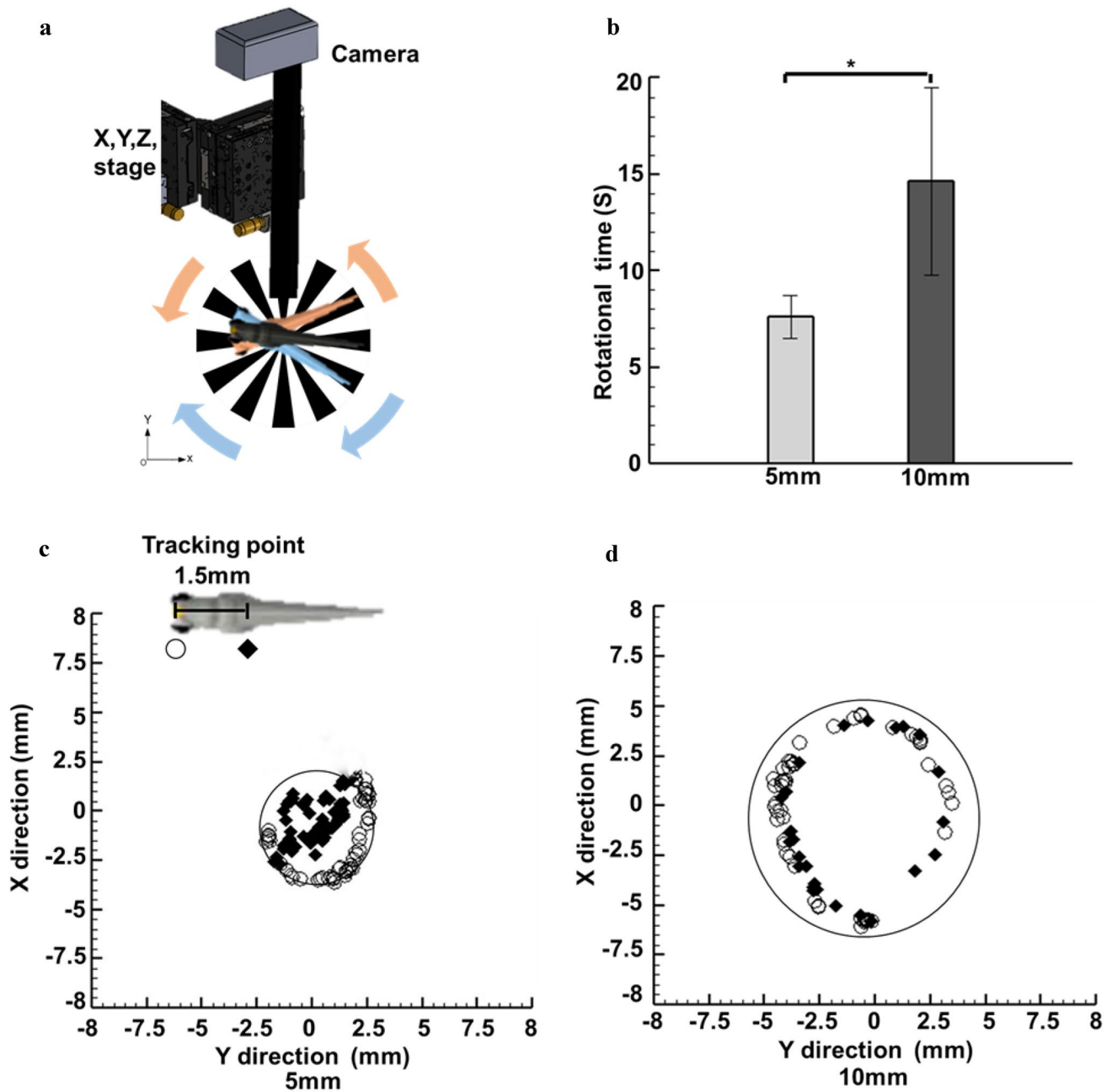


**Fig. 5** OKR responses to mediated self-orientation of the larvae to the camera axis. **a** Schematic illustration of the larvae dynamics through light pattering, **b** the average traversing time required for axial rotation of larvae under stimuli for a complete rotational cycle for 5 d.p.f. zebrafish larvae with the optimal grating frequency of

1.5 Hz and a grating width ratio of 1:1. Error bars denote one standard deviation over seven zebrafish; \**p* value < 0.01 for the paired sample *t* tests, and the tracking point on the larvae (direction specific) orientation correspondence to rotational stimuli. **c** Trajectories of the selected points in 5-mm (**c**) and 10-mm (**d**) test sections

**Acknowledgments** This study was supported through the Ministry of Science and Technology of Taiwan under Contract No. MOST 108-2221-E-006-221-MY4 (to Chia-Yuan Chen). This work would not be possible without the facility provided by Center for Micro/Nano Science and Technology, National Cheng Kung University. This research was supported in part by the Higher Education Sprout Project, Ministry of Education to the Headquarters of University Advancement at National Cheng Kung University.

## References

Agrawal AA (2001) Phenotypic plasticity in the interactions and evolution of species. *Science* 294:321–326. <https://doi.org/10.1126/science.1060701>

Asnani A, Peterson RT (2014) The zebrafish as a tool to identify novel therapies for human cardiovascular disease. *Dis Models Mech* 7:763–767

- Blaser RE, Chadwick L, McGinnis GC (2010) Behavioral measures of anxiety in zebrafish (*Danio rerio*). *Behav Brain Res* 208:56–62. <https://doi.org/10.1016/j.bbr.2009.11.009>
- Brockerhoff SE (2006) Measuring the optokinetic response of zebrafish larvae. *Nat Protoc* 1:2448–2451. <https://doi.org/10.1038/nprot.2006.255>
- Chang TY, Pardo-Martin C, Allalou A, Wahlby C, Yanik MF (2012) Fully automated cellular-resolution vertebrate screening platform with parallel animal processing. *Lab Chip* 12:711–716
- Chen C-Y, Chang Chien T-C, Mani K, Tsai H-Y (2016) Axial orientation control of zebrafish larvae using artificial cilia. *Microfluid Nanofluid* 20:12. <https://doi.org/10.1007/s10404-015-1668-z>
- Chen C-Y, Chen C-Y, Lin C-Y, Hu Y-T (2013) Magnetically actuated artificial cilia for optimum mixing performance in microfluidics. *Lab Chip* 13:2834–2839
- Condon CH, Chenoweth SF, Wilson RS (2010) Zebrafish take their cue from temperature but not photoperiod for the seasonal plasticity of thermal performance. *J Exp Biol* 213:3705–3709. <https://doi.org/10.1242/jeb.046979>
- Cortemeglia C, Beitinger TL (2005) Temperature tolerances of wild-type and red transgenic zebra danios. *Trans Am Fish Soc* 134:1431–1437. <https://doi.org/10.1577/T04-197.1>
- Dooley K, Zon LI (2000) Zebrafish: a model system for the study of human disease. *Curr Opin Genet Dev* 10:252–256
- Emran F, Rihel J, Dowling JE (2008) A behavioral assay to measure responsiveness of zebrafish to changes in light intensities. *J Vis Exp* 923. <https://doi.org/10.3791/923>
- Engeszer RE, Patterson LB, Rao AA, Parichy DM (2007) Zebrafish in the wild: a review of natural history and new notes from the field. *Zebrafish* 4:21–40. <https://doi.org/10.1089/zeb.2006.9997>
- Harper C, Lawrence C (2010) *The laboratory Zebrafish*. CRC Press, Boca Raton, p 274
- Kimmel CB, Ballard WW, Kimmel SR, Ullmann B, Schilling TF (1995) Stages of embryonic development of the zebrafish. *Dev Dyn* 203:253–310. <https://doi.org/10.1002/aja.1002030302>
- Lawrence C (2007) The husbandry of zebrafish (*Danio rerio*): a review. *Aquaculture* 269:1–20. <https://doi.org/10.1016/j.aquaculture.2007.04.077>
- Li Y et al (2014) Zebrafish on a chip: a novel platform for real-time monitoring of drug-induced developmental toxicity. *PLoS ONE* 9:e94792. <https://doi.org/10.1371/journal.pone.0094792>
- Lin X et al (2015) High-throughput mapping of brain-wide activity in awake and drug-responsive vertebrates. *Lab Chip* 15:680–689
- Mani K, Chang Chien T-C, Panigrahi B, Chen C-Y (2016) Manipulation of zebrafish's orientation using artificial cilia in a microchannel with actively adaptive wall design. *Sci Rep* 6:36385
- Mani K, Hsieh Y-C, Panigrahi B, Chen C-Y (2018) A noninvasive light driven technique integrated microfluidics for zebrafish larvae transportation. *Biomicrofluidics* 12:021101–021101
- Marks C, West TN, Bagatto B, Moore FBG (2005) Developmental Environment Alters Conditional Aggression in Zebrafish. *Copeia* 2005:901–908. [https://doi.org/10.1643/0045-8511\(2005\)005\[0901:DEACAI\]2.0.CO;2](https://doi.org/10.1643/0045-8511(2005)005[0901:DEACAI]2.0.CO;2)
- Neuhauss SC (2003) Behavioral genetic approaches to visual system development and function in zebrafish. *Dev Neurobiol* 54:148–160
- Panigrahi B, Chen C-Y (2019a) microfluidic transportation control of larval zebrafish through optomotor regulations under the pressure-driven flow. *Micromachines* 10(12):880
- Panigrahi B, Chen C-Y (2019b) Microfluidic retention of progressively motile zebrafish sperms. *Lab Chip* 19:4033–4042. <https://doi.org/10.1039/C9LC00534J>
- Ruiz-Oliveira J, Silva PF, Luchiaro AC (2019) Coffee time: low caffeine dose promotes attention and focus in zebrafish. *Learn Behav* 47:227–233. <https://doi.org/10.3758/s13420-018-0369-3>
- Sawant MS, Zhang S, Li L (2011) Effect of salinity on development of zebrafish, *Brachydanio rerio*. *Res Commun* 81
- Schaefer JF, Ryan A (2006) Developmental plasticity in the thermal tolerance of zebrafish *Danio rerio*. *J Fish Biol* 69:722–734. <https://doi.org/10.1111/j.1095-8649.2006.01145.x>
- Schindelin J et al (2012) Fiji: an open-source platform for biological-image analysis. *Nat Methods* 9:676–682
- Schmitt EA, Dowling JE (1999) Early retinal development in the zebrafish, *Danio rerio*: light and electron microscopic analyses. *J Comp Neurol* 404:515–536
- Scott GR, Johnston IA (2012) Temperature during embryonic development has persistent effects on thermal acclimation capacity in zebrafish. *Proc Natl Acad Sci* 109:14247. <https://doi.org/10.1073/pnas.1205012109>
- Son SU, Garrell RL (2009) Transport of live yeast and zebrafish embryo on a droplet (“digital”) microfluidic platform. *Lab Chip* 9:2398–2401. <https://doi.org/10.1039/B906257B>
- Steele WB, Mole RA, Brooks BW (2018) Experimental protocol for examining behavioral response profiles in larval fish: application to the neuro-stimulant caffeine. *J Vis Exp*. <https://doi.org/10.3791/57938>
- Stewart A et al (2011) Zebrafish models to study drug abuse-related phenotypes. *Rev Neurosci* 22:95–105. <https://doi.org/10.1515/RNS.2011.011>
- Vestergaard P (2008) Skeletal effects of central nervous system active drugs: anxiolytics, sedatives, antidepressants, lithium and neuroleptics. *Curr Drug Saf* 3:185–189. <https://doi.org/10.2174/157488608785699432>
- Via S, Lande R (1985) Genotype-environment interaction and the evolution of phenotypic plasticity. *Evolution* 39:505–522. <https://doi.org/10.1111/j.1558-5646.1985.tb00391.x>
- Villamizar N, Vera LM, Foulkes NS, Sánchez-Vázquez FJ (2014) Effect of lighting conditions on zebrafish growth and development. *Zebrafish* 11:173–181. <https://doi.org/10.1089/zeb.2013.0926>
- Wielhouwer EM et al (2011) Zebrafish embryo development in a microfluidic flow-through system. *Lab Chip* 11:1815–1824. <https://doi.org/10.1039/C0LC00443J>
- Wolf S et al (2017) Sensorimotor computation underlying phototaxis in zebrafish. *Nat Commun* 8:651
- Yang F, Gao C, Wang P, Zhang G-J, Chen Z (2016) Fish-on-a-chip: microfluidics for zebrafish research. *Lab Chip* 16:1106–1125. <https://doi.org/10.1039/C6LC00044D>
- Zhang Q, Kopp M, Babiak I, Fernandes JMO (2018) Low incubation temperature during early development negatively affects survival and related innate immune processes in zebrafish larvae exposed to lipopolysaccharide. *Sci Rep* 8:4142. <https://doi.org/10.1038/s41598-018-22288-8>
- Zheng C, Zhou H, Liu X, Pang Y, Zhang B, Huang Y (2014) Fish in chips: an automated microfluidic device to study drug dynamics in vivo using zebrafish embryos. *Chem Commun* 50:981–984. <https://doi.org/10.1039/C3CC47285J>

**Publisher's Note** Springer Nature remains neutral with regard to jurisdictional claims in published maps and institutional affiliations.